inorganics

MDPI

Article

Diameter-Selective Host-Guest Interactions between Functionalized Fullerenes and Single-Walled Carbon Nanotubes

Rui Zhang [1,2], Wanru Gao [2], Chang Sun [2], Yiwen Liu [1], Xiaojun Lu [1,*] and Xing Lu [2,*]

[1] Key Laboratory for Green Chemical Process of Ministry of Education, School of Chemical Engineering and Pharmacy, Wuhan Institute of Technology, Wuhan 430205, China; ruizhang@wit.edu.cn (R.Z.); liuyw10725@163.com (Y.L.)

[2] State Key Laboratory of Materials Processing and Die & Mould Technology, School of Materials Science and Engineering, Huazhong University of Science and Technology, Wuhan 430074, China; m201470729@hust.edu.cn (W.G.); m201470762@hust.edu.cn (C.S.)

* Correspondence: xiaojunlu.sa@outlook.com (X.L.); lux@hust.edu.cn (X.L.)

Abstract: Carbon nano peapods, with their electronic properties and spintronics, have attracted great attention regarding their potential applications when combined with fullerenes or their derivatives encapsulated inside. Herein, we have designed and synthesized a series of fullerene derivatives with different functional groups, which are then encapsulated into single-walled carbon nanotubes (SWCNTs). Accurate morphological characterization with high-resolution TEM reveals a clear correlation between the filling ratio of the peapods and the steric bulk of the functionalized groups. Further spectroscopic characterizations reveal diameter-selective interactions between the fullerene derivatives and SWCNTs, which, in turn, influence the electronic structures of the nanotubes. Our results have shed new light on the controlled synthesis and property-tuning of nano peapods.

Keywords: peapod; carbon nanotubes; fullerenes; fullerene derivatives

Citation: Zhang, R.; Gao, W.; Sun, C.; Liu, Y.; Lu, X.; Lu, X. Diameter-Selective Host-Guest Interactions between Functionalized Fullerenes and Single-Walled Carbon Nanotubes. *Inorganics* **2023**, *11*, 386. https://doi.org/10.3390/inorganics11100386

Academic Editor: Duncan H. Gregory

Received: 10 August 2023
Revised: 22 September 2023
Accepted: 22 September 2023
Published: 27 September 2023

1. Introduction

Since the discovery of a new type of hybrid carbon nanostructure, with fullerenes inside carbon nanotubes (CNTs), the so-called peapods [1], a range of hollow fullerenes [2–4] and metallofullerenes [5–8], have been encapsulated into SWCNTs. Accordingly, carbon nanotubes acting as nano-containers [9] and nano-reactors [10] have become a hot topic in terms of the exploitation and modification of their excellent electronic [11] and mechanical properties [12] in nanomaterial science. It is well established that the fullerene dopants can modify the electronic structures of SWCNTs [13–15] and lead to advantageous physical and chemical properties that could be utilized in many applications, such as nanoelectronics [16,17], quantum computing [15,18], and thermoelectricity [19,20].

It has gradually become understood that the unprecedented properties and functions of peapods are due largely to the interactions between fullerenes and SWCNTs induced by the attractive physical and chemical properties of the encapsulated fullerenes. More importantly, the exteriors of fullerene molecules can be involved in organic reactions, facilitating the attachment of functional groups to their carbon cages and thereby imparting numerous distinct properties. As a consequence, the fullerene cages serve as vehicles for transferring some electrostatically bonded complexes into carbon nanotubes, which exert a shielding effect on the optical properties of the guest molecules, such as emission quenching [21,22]. This means that the combination of functionalized fullerenes with unique properties and SWCNTs holds paramount significance. However, the previous studies into the encapsulation of functionalized fullerenes into SWCNTs have focused mainly on the control of specific orientations and the packing of molecules inside SWCNTs, as observed via high-resolution TEM [23–25]. The interactions between different fullerene

derivatives and SWCNTs in their peapod structures, which are closely related to the resultant properties of the peapods, are yet to be systematically studied.

In this work, pristine C_{60} and three C_{60}-derivatives (**1**, **2** and **3**) containing different functional groups [23] have been successfully inserted into SWCNTs. The structural diagrams of are depicted in Figure 1. Our results reveal that the filling ratio of the resultant peapods decreases with the increasing steric bulk of the addends. More importantly, we confirm, for the first time, that the encapsulation of these fullerene derivatives is highly dependent on the diameter of the SWCNTs, as evidenced via the Raman and UV spectroscopic results.

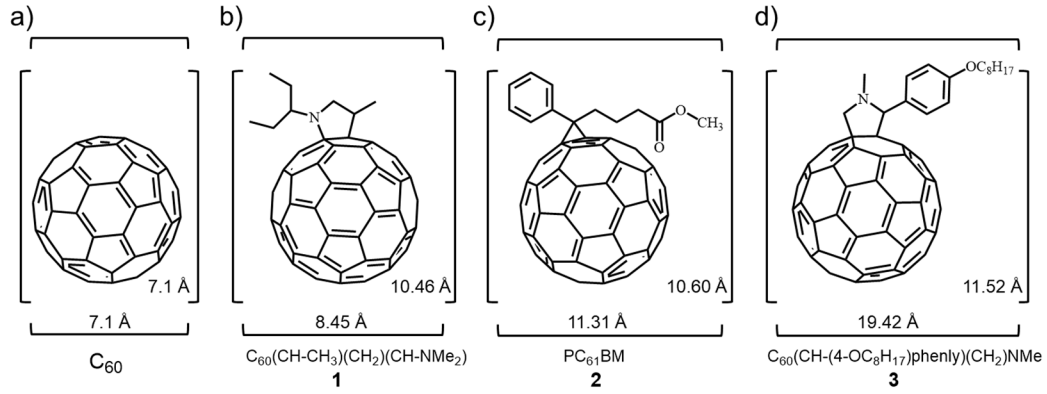

Figure 1. Structural diagrams of C_{60} (**a**) and its derivatives **1** (**b**), **2** (**c**) and **3** (**d**).

2. Results and Discussion

The resultant peapod structures with C_{60}, **1**, **2** and **3** inside SWCNTs are first investigated via HR-TEM (Figure 2). Meanwhile, based on the synthesis procedures of peapods, no other substance other than C_{60}, **1**, **2** and **3** could contribute a round shape in the HR-TEM images, suggesting the successful encapsulation of the fullerene dopants inside SWCNTs. Moreover, we have roughly estimated the filling rate of peapods as being above 80% via HR-TEM observation (Figure S13 in Supplementary Materials). It appears that the filling ratio of the peapods decreases along with the increasing bulk of the addends in these hybrids, possibly due to the increasing steric hindrance of the functional groups. Moreover, the derivatives (**1**, **2** and **3**) exhibit largely disordered arrangements, with larger inter-fullerene spacing inside SWCNTs (Figure 2b–d) than that of C_{60}@SWCNT peapods (Figure 2a). In particular, the short and rigid organic group attaching to the fullerene cage is clearly seen in the **1**@SWCNT peapods (Figure 2b). Furthermore, it has been observed that the substantial size of the side group in compound **3** impedes its encapsulation within the SWCNT, and leads, instead, to a conspicuous attachment onto the external surface of the nanotubes, adopting folded conformations (Figure 2d). In contrast, the attachment of the fullerene moiety on the surface of the SWCNT is not obvious in C_{60}@SWCNT, **1**@SWCNT, and **2**@SWCNT, but these fullerene derivatives are largely encapsulated. These results confirm a size effect of the side group of fullerene derivatives on the encapsulation ratio and even the attachment on the SWCNT surface. Moreover, a collapse in the fullerene entities is observed in **1**@SWCNT, **2**@SWCNT, and **3**@SWCNT (Figure 2b–d), but the spherical structure of C_{60} is rather intact, as found in C_{60}@SWCNT. These results indicate that the functionalized derivatives (**1**, **2** and **3**) are less stable than pristine C_{60} under electron beam irradiation.

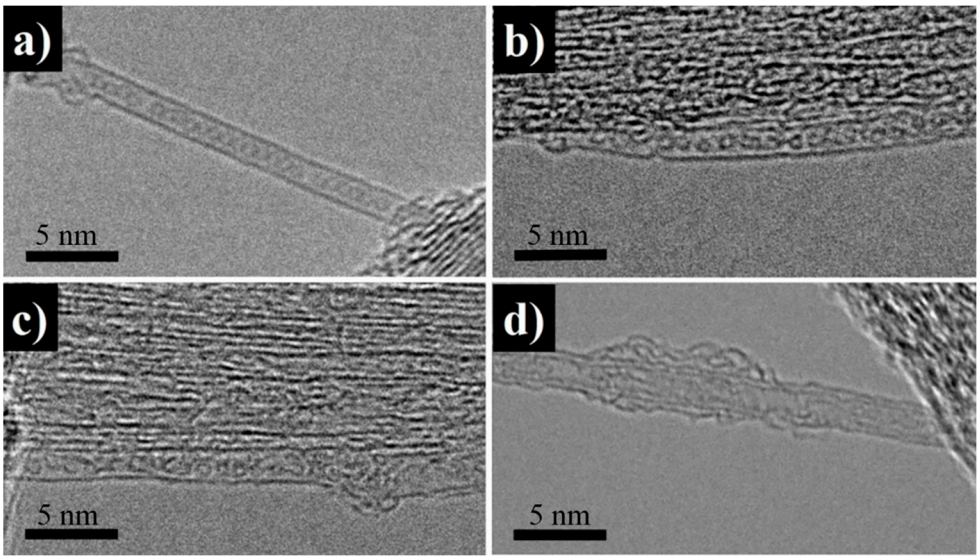

Figure 2. HR-TEM images of (**a**) C_{60}@SWNTs, (**b**) **1**@SWNTs, (**c**) **2**@SWNTs, and (**d**) **3**@SWNTs.

The Raman spectroscopic characterization of empty SWCNT, C_{60}@SWCNT, **1**@SWCNT, **2**@SWCNT, and **3**@SWCNT peapods is carried out to study the interactions between the fullerene moieties and SWCNTs. It is obvious that the encapsulation of these C_{60}-molecules does not cause any additional structural damage to the nanotubes because of the nearly identical intensity of the D bands (1342 cm^{-1}) for the above four samples (Figure 3a). In addition, there is a slight broadening of the G-bands (1572 cm^{-1}) of the doped nanotubes (Figure S9), especially in C_{60}@SWCNTs and **1**@SWNTs, which further confirms the high filling ratio and strong interactions between the dopants and SWCNTs [26].

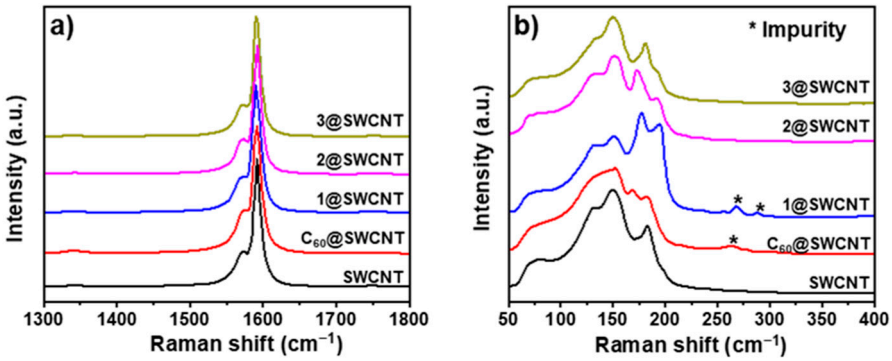

Figure 3. Raman spectra of the C_{60}@SWCNT, **1**@SWCNT, **2**@SWCNT, and **3**@SWCNT peapods and empty SWCNTs in the ranges of (**a**) 1300–1800 cm^{-1} (D bands and G bands) and (**b**) 50–400 cm^{-1} (RBM bands). The Raman spectra were obtained with an excitation wavelength of 532 nm, at room temperature.

The Raman results in the radial-breathing-mode (RBM) region reveal that the mutual interactions between fullerene moieties and SWCNTs are highly diameter-selective in the samples under study (Figure 3b and Table 1) [27]. The un-doped SWCNTs display typical RBM peaks corresponding to the diameters of 1.89 nm, 1.65 nm, and 1.35 nm, respectively. After encapsulation, the peaks corresponding to the samples with a diameter of either ~1.89 nm or ~1.65 nm are unchanged, indicating that the encapsulation of C_{60}, **1**, **2** and **3** does not affect strongly the vibrations of these large nanotubes because of weak inter–outer interactions. We can, thus, speculate that the effect of the suppression between the encapsulated fullerenes and SWCNTs is probably the major reason for the unchanged resonant condition of the doped SWCNTs. However, the peak at 183 cm^{-1}, corresponding to a diameter of 1.35 nm for the pristine SWCNTs, is obviously shifted for the doped

samples. To expand, a new peak at 172 cm^{-1} (1.44 nm) is observed for C_{60}@SWCNTs, and new peaks in a range from 175 cm^{-1} (1.42 nm) to 191 cm^{-1} (1.27 nm) are found for another three peapods. According to the relevant research, it is customary to assess the successful formation of peapods by scrutinizing the emergence of distinct signals within the Raman spectra of the peapod systems [28,29]. These results clearly confirm the diameter-selective interactions between the fullerene derivatives and SWCNTs. In particular, the appearance of RBM peaks corresponding to a diameter of about 1.40 nm is attributed to interactions between the SWCNTs and the encapsulated fullerenes (C_{60}, **1**, 2 and **3**) inside the nanotubes, while the interactions between SWCNTs and the functionalized fullerenes attached to the outer surfaces of nanotubes lead to the appearance of RBM peaks corresponding to a diameter below 1.30 nm. The appearance of these new RBM peaks provides strong evidence of the diameter-selective interactions between SWCNTs and the functionalized fullerenes inside and outside the nanotubes [30].

Table 1. The positions of the RBM peaks for the SWCNTs before and after the encapsulation of C_{60}, **1**, **2** and **3** (the values in parentheses are the diameters of the corresponding tubes, calculated via the RMB peaks, using the equation D (nm) = 248/ω).

Samples	The RBM Peaks (cm^{-1}) and Calculated Diameters (nm) of the SWCNTs				
SWCNT	131.22 (1.89)	150.30 (1.65)		183.70 (1.35)	
C_{60}@SWCNT	131.22 (1.89)	152.15 (1.63)	172.22 (1.44)	183.70 (1.35)	
1@SWCNT	131.22 (1.89)	151.22 (1.64)	178.42 (1.39)		195.28 (1.27)
2@SWCNT	131.22 (1.89)	162.22 (1.64)	174.64 (1.42)		190.77 (1.30)
3@SWCNT	131.22 (1.89)	149.40 (1.66)		181.02 (1.37)	195.28 (1.27)

The UV-Vis-NIR spectroscopic results for the empty SWCNTs, C_{60}@SWCNTs, **1**@SWCNTs, **2**@SWCNTs, and **3**@SWCNTs, together with the corresponding precursors (C_{60}, **1**, **2** and **3**), are shown in Figure 4 (Figures S8 and S10–S12), to allow further investigation of the inner–outer interactions. The precursors (C_{60}, **1**, **2** and **3**) dissolved in CS_2 display strong bands at around 330 nm, with a characteristic absorption peak at about 430 nm for the [6,6]-addition patterns in **1**, **2** and **3** [13,31]. However, these characteristic peaks disappear completely after encapsulation inside nanotubes, indicating a shielding effect of the π-system of SWCNTs on the absorption of fullerene derivatives. Upon encapsulating fullerene derivatives, the peapods exhibit a significant broadening of approximately ~13 nm and a blue shift of approximately ~10 nm at the absorption band of 300–400 nm, compared to pristine SWCNTs (Figure 4b), suggesting that the encapsulated fullerenes have an obvious influence on the electronic structure of the SWCNTs.

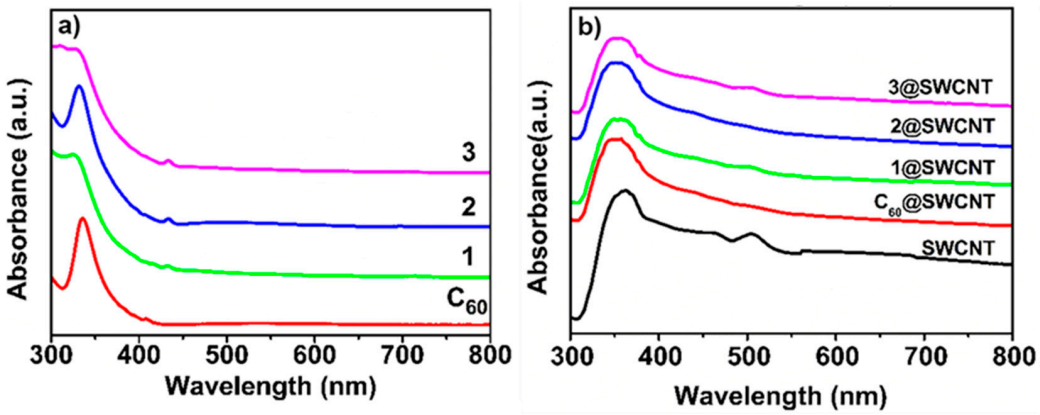

Figure 4. UV-Vis absorption spectra of (**a**) C_{60}, **1**, **2** and **3** dissolved in CS_2; (**b**) **1**@SWCNTs, **2**@SWCNTs, **3**@SWCNTs, C_{60}@SWCNTs, and empty SWCNTs dispersed in ethanol.

3. Materials and Methods

3.1. Purification of SWCNTs

The deuterated chloroform (99.8%) was supplied by J&K Chemical Limited. The other chemicals and solvents were purchased from Sinopharm Chemical Reagent Co., Ltd. All the chemicals and reagents were used without further purification.

The SWCNT samples, with a purity of 75 wt%, were supplied by OCSiAl Ltd. The as-received SWCNT samples were heated at 350 °C in air for 30 min, and then were refluxed in a mixed solution of $K_2S_2O_8$ (0.2 mol/L) and sulfuric acid (98%), with a volume ratio of 6:1, at 60 °C for 24 h. The resulting samples were washed with hydrochloric acid to further remove metal impurities. The high purity over 90% of the resulting SWCNTs was verified via TGA and Raman spectra (Figure S1a,b). The diameter distribution of the SWCNTs was estimated to be in the range of 1.27 nm–2.05 nm via Raman spectroscopy and HR-TEM observation. The oxidation treatment opened the ends and led to some defects along the walls of the SWCNTs, which guaranteed sufficient entrances and facilitated the encapsulation process of the fullerene derivatives. However, the exposed nanotube ends were also functionalized with carboxylic groups to go against the efficient encapsulation of fullerenes [32,33], which should be eliminated prior to the encapsulation process. To this end, the purified SWCNTs were conducted with a heat treatment at 500 °C for 30 min in air to ensure sufficient holes and the decomposition of carboxylic groups. The resulting SWCNTs were kept at 120 °C to get rid of water and were taken out immediately prior to the encapsulation process.

3.2. Synthesis of **1**, **2** *and* **3**

The fullerene derivative **1** $C_{60}(C_6H_{15}N)$ (Figures S2 and S3) was synthesized according to a previously reported procedure [31]; the fullerene derivative **2** $C_{60}(C_{12}H_{14}O_2)$, $PC_{61}BM$ (>99.5%, HPLC) was purchased from Luminescence Technology Corp; the fullerene derivative **3** $C_{60}(C_{17}H_{27}NO)$ was prepared according to the procedure outlined in Scheme 1.

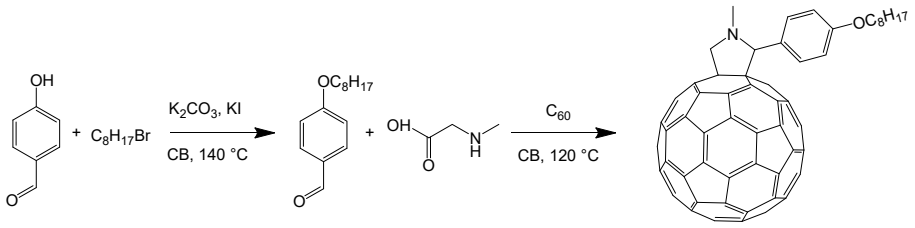

Scheme 1. The synthetic procedure for derivative **3**.

To explain further, a solution of C_{60} (720 mg, 1 mmol) (Figures S6 and S7) in 150 mL chlorobenzene was mixed with 4-(octyloxy) benzaldehyde (936 mg, 4 mmol) and sarcosine (268 mg, 3 mmol) in 20 mL chlorobenzene, and the reaction mixture was heated at 120 °C under an argon atmosphere. The whole reaction process was monitored via HPLC (Figure S4). In the beginning, the two peaks corresponding to the solvent and C_{60} appeared at 4.3 min and 7.9 min, respectively, indicating that no reaction had taken place. After 60 min, the peak of the desired product **3** appeared at 4.7 min, and the peak intensity continued to increase along with the increasing reaction time. The reaction was terminated after 300 min revealing a significant increase in the intensity of the product peak, accompanied by a notable attenuation of the starting material peak. Simultaneously, peaks indicative of bis- or multi-adducts were observed. Finally, the reaction mixture was separated via HPLC, which gave **3** (Figure S5) in a yield of 68% based on the consumed C_{60}.

3.3. Characterizations

High-resolution transmission electron microscopy (HR-TEM) observations were performed with a FEI Tecnai G2F20 S-TWIN at an acceleration voltage of 200 kV. The imaging conditions were set to minimize the irradiation damage as much as possible. The specimens

were suspended in ethanol (99.9 vol.%) via sonication and then dropped onto a copper microgrid. Raman spectra were collected using a LabRAM HR800 spectrometer and measured via random selection with a laser excitation wavelength of 532 nm in ambient conditions. The suspensions of peapods in ethanol were added dropwise onto the microslide, resulting in film samples. UV–visible–near-infrared (UV-Vis-NIR) spectra were recorded using a PE Lambda 750S spectrophotometer, with a wavelength range of 300–800 nm for the fullerenes and their derivatives dissolved in CS_2, and of 300–2000 nm for the empty and doped SWCNTs dispersed in ethanol (the results for the peapods dispersed into D_2O with surfactants such as sodium cholate, sodium deoxycholate, and sodium dodecylbenzenesulfonate were quite similar to those for ethanol). The isolation of C_{60} and its derivatives was conducted via preparative high-performance liquid chromatography (HPLC) with an LC-9130 NEXT instrument, using toluene as an eluent. MALDI-TOF mass spectra were measured using a BIFLEX III spectrometer, with 1,1,4,4-tetraphenyl-1,3-butadiene as the matrix. ^{1}H and ^{13}C NMR spectra were recorded in deuterated chloroform at 600 MHz and 151 MHz, respectively. Chemical shifts (δ) were given in ppm relative to the solvent, and the coupling constants (J) were given in Hz. Thermal gravimetric analysis (TGA) was performed under air flow from the ambient temperature to 800 °C, at a heating rate of 10 °C/min.

4. Conclusions

In conclusion, we successfully encapsulated C_{60} and its three derivatives into SWCNTs to obtain the corresponding peapod structures. Our findings indicate that the filling ratio of peapods evidently relies on the steric bulk of the functional group of the derivatives. Moreover, Raman spectroscopic characterizations illuminate that the selective appearance of the RBM peaks of the doped SWCNTs is clearly associated with the diameter-selective interactions between SWCNTs and the functionalized fullerenes both inside and outside nanotubes. It is further confirmed that the encapsulation of functionalized fullerenes directly affects the electronic structure of SWCNTs via UV-Vis-NIR absorption spectra. Our study exposes the relationship of the interactions between the functionalized fullerenes and SWCNTs in hybrid peapod structures. We expect that the insights gained in this investigation may provide future theoretical works for designing controllable synthesis of, and good properties in, nano peapods. Our results have shed new light on the controlled synthesis and property-tuning of nano peapods.

Supplementary Materials: The following supporting information can be downloaded at: https://www.mdpi.com/article/10.3390/inorganics11100386/s1, Figure S1. Thermal gravimetric analysis for SWCNTs after multi-step purification (a). The Raman spectra of SWCNTs (b); Figure S2. HPLC profiles of the reaction mixture between C_{60} and triethylamine probed at different times at 140 °C. Conditions: Buckyprep column (Φ4.6 mm × 250 mm), toluene eluent; flow rate 1.0 mL/min, detection wavelength 330 nm; Figure S3. MALDI-TOF mass spectrum of functionalized fullerene **1**; Figure S4. HPLC profiles of the reaction mixture between C_{60} and 4-(octyloxy) benzaldehyde probed at different times at 120 °C. Conditions: Buckyprep column (Φ4.6 mm × 250 mm), toluene eluent; flow rate 1.0 mL/min, detection wavelength 290 nm; Figure S5. MALDI-TOF mass spectrum of functionalized fullerene **3**; Figure S6. MALDI-TOF mass spectrum for C_{60}; Figure S7. Raman spectra of C_{60}; Figure S8. The log–log UV-Vis absorption spectra of (a) C_{60}, **1**, **2** and **3** dissolved in CS_2; (b) **1**@SWCNTs, **2**@SWCNTs, **3**@SWCNTs, C_{60}@SWCNTs, and empty SWCNTs dispersed in ethanol. Normalized UV-Vis absorption spectra of (c) C_{60}, **1**, **2** and **3** dissolved in CS_2; (d) **1**@SWCNTs, **2**@SWCNTs, **3**@SWCNTs, C_{60}@SWCNTs, and empty SWCNTs dispersed in ethanol; Figure S9. Raman spectra of C_{60}@SWCNT, **1**@SWCNT, **2**@SWCNT, and **3**@SWCNT peapods and empty SWCNTs in the range of 1500–1700 cm^{-1}; Figure S10. UV-Vis absorption spectra of (a) the double-walled carbon nanotubes found in [34] and (b) the SWCNTs and peapods in this work. The dashed red arrows indicate the absorption band at around 300–400 nm; Figure S11. UV-Vis absorption spectra of (a) the SWCNTs found in [35] and (b) the SWCNTs and peapods in this work. The dashed red arrows indicate the absorption band at around 500 nm; Figure S12. UV-Vis absorption spectra of (a) **2**, **2**@SWCNT, and SWCNT; (b) **2**; Figure S13. The HR-TEM results of (a) the C_{60}@SWCNT peapods and (b) the C_{60}@SWCNTs prepared via large-diameter SWCNTs (1.79~2.05 nm) are included.

Author Contributions: Conceptualization, W.G. and R.Z.; methodology, C.S. and W.G.; validation, R.Z. and Y.L.; formal analysis, W.G. and R.Z.; investigation, W.G.; data curation, R.Z.; writing—original draft preparation, R.Z. and W.G.; writing—review and editing, R.Z.; visualization, W.G. and R.Z.; supervision, X.L. (Xing Lu) and X.L. (Xiaojun Lu); project administration, X.L. (Xing Lu); funding acquisition, X.L. (Xing Lu) and R.Z. All authors have read and agreed to the published version of the manuscript.

Funding: This study was financially supported by the National Natural Science Foundation of China (No. 21925104), the Hubei Key Laboratory of Novel Reactor and Green Chemical Technology (No. NRGC202208), and the Start-up Funding of Wuhan Institute of Technology (No. 21QD08).

Data Availability Statement: The data presented in this study are available on request from the corresponding author.

Conflicts of Interest: The authors declare no conflict of interest.

References

1. Smith, B.W.; Monthioux, M.; Luzzi, D.E. Encapsulated C_{60} in Carbon Nanotubes. *Nature* **1998**, *396*, 323–324. [CrossRef]
2. Fakrach, B.; Fergani, F.; Boutahir, M.; Rahmani, A.; Chadli, H.; Hermet, P.; Rahmani, A. Structure and Raman Spectra of C_{60} and C_{70} Fullerenes Encased into Single-Walled Boron Nitride Nanotubes: A Theoretical Study. *Crystals* **2018**, *8*, 118. [CrossRef]
3. Cao, J.; Wang, Y.; Chai, J.; Shi, J. Nano-Peapods from C_{60}-Encapsulated CNTs Driving Self-Assembly of Phosphorus Nanotube: A Molecular Dynamics Study. *Comput. Mater. Sci.* **2019**, *160*, 403–410. [CrossRef]
4. Nishimura, M.; Hatta, M. Local Buckling Behavior of Multi-Walled Carbon Nanotubes Encapsulating C_{60} Fullerenes. *Carbon Trends* **2023**, *11*, 100269. [CrossRef]
5. Kodama, T.; Ohnishi, M.; Park, W.; Shiga, T.; Park, J.; Shimada, T.; Shinohara, H.; Shiomi, J.; Goodson, K.E. Modulation of Thermal and Thermoelectric Transport in Individual Carbon Nanotubes by Fullerene Encapsulation. *Nat. Mater* **2017**, *16*, 892–897. [CrossRef]
6. Nakanishi, R.; Satoh, J.; Katoh, K.; Zhang, H.; Breedlove, B.K.; Nishijima, M.; Nakanishi, Y.; Omachi, H.; Shinohara, H.; Yamashita, M. $DySc_2N@C_{80}$ Single-Molecule Magnetic Metallofullerene Encapsulated in a Single-Walled Carbon Nanotube. *J. Am. Chem. Soc.* **2018**, *140*, 10955–10959. [CrossRef]
7. Okazaki, T.; Suenaga, K.; Hirahara, K.; Bandow, S.; Iijima, S.; Shinohara, H. Electronic and Geometric Structures of Metallofullerene Peapods. *Phys. B Condens. Matter* **2002**, *323*, 97–99. [CrossRef]
8. Sato, Y.; Suenaga, K.; Okubo, S.; Okazaki, T.; Iijima, S. Structures of D_{5d}-C_{80} and I_h-$Er_3N@C_{80}$ Fullerenes and Their Rotation Inside Carbon Nanotubes Demonstrated by Aberration-Corrected Electron Microscopy. *Nano Lett.* **2007**, *7*, 3704–3708. [CrossRef]
9. Sloan, J.; Dunin-Borkowski, R.E.; Hutchison, J.L.; Coleman, K.S.; Clifford Williams, V.; Claridge, J.B.; York, A.P.E.; Xu, C.; Bailey, S.R.; Brown, G.; et al. The Size Distribution, Imaging and Obstructing Properties of C_{60} and Higher Fullerenes Formed within Arc-Grown Single Walled Carbon Nanotubes. *Chem. Phys. Lett.* **2000**, *316*, 191–198. [CrossRef]
10. Wilson, M.; Madden, P.A. Growth of Ionic Crystals in Carbon Nanotubes. *J. Am. Chem. Soc.* **2001**, *123*, 2101–2102. [CrossRef]
11. Kavan, L.; Dunsch, L.; Kataura, H.; Oshiyama, A.; Otani, M.; Okada, S. Electrochemical Tuning of Electronic Structure of C_{60} and C_{70} Fullerene Peapods: In Situ Visible Near-Infrared and Raman Study. *J. Phys. Chem. B* **2003**, *107*, 7666–7675. [CrossRef]
12. Yang, X.; Yao, M.; Wu, X.; Liu, S.; Chen, S.; Yang, K.; Liu, R.; Cui, T.; Sundqvist, B.; Liu, B. Novel Superhard Sp^3 Carbon Allotrope from Cold-Compressed C_{70} Peapods. *Phys. Rev. Lett.* **2017**, *118*, 245701. [CrossRef] [PubMed]
13. Okazaki, T.; Okubo, S.; Nakanishi, T.; Joung, S.-K.; Saito, T.; Otani, M.; Okada, S.; Bandow, S.; Iijima, S. Optical Band Gap Modification of Single-Walled Carbon Nanotubes by Encapsulated Fullerenes. *J. Am. Chem. Soc.* **2008**, *130*, 4122–4128. [CrossRef]
14. Yang, J.; Lee, J.; Lee, J.; Yi, W. Conductivity and Field Emission Enhancement of C_{60}-Encapsulated Single-Walled Carbon Nanotubes. *Diam. Relat. Mater.* **2018**, *89*, 273–281. [CrossRef]
15. Matsuno, T.; Terasaki, S.; Kogashi, K.; Katsuno, R.; Isobe, H. A Hybrid Molecular Peapod of Sp^2- and Sp^3-Nanocarbons Enabling Ultrafast Terahertz Rotations. *Nat. Commun.* **2021**, *12*, 5062. [CrossRef]
16. Lee, J.; Kim, H.; Kahng, S.-J.; Kim, G.; Son, Y.-W.; Ihm, J.; Kato, H.; Wang, Z.W.; Okazaki, T.; Shinohara, H.; et al. Bandgap Modulation of Carbon Nanotubes by Encapsulated Metallofullerenes. *Nature* **2002**, *415*, 1005–1008. [CrossRef]
17. Kuznetsov, V. Stereochemistry of Simple Molecules inside Nanotubes and Fullerenes: Unusual Behavior of Usual Systems. *Molecules* **2020**, *25*, 2437. [CrossRef]
18. Hornbaker, D.J.; Kahng, S.-J.; Misra, S.; Smith, B.W.; Johnson, A.T.; Mele, E.J.; Luzzi, D.E.; Yazdani, A. Mapping the One-Dimensional Electronic States of Nanotube Peapod Structures. *Science* **2002**, *295*, 828–831. [CrossRef]
19. Rodríguez Méndez, Á.; Medrano Sandonas, L.; Dianat, A.; Gutierrez, R.; Cuniberti, G. An Atomistic Study of the Thermoelectric Signatures of CNT Peapods. *J. Phys. Chem. C* **2021**, *125*, 13721–13731. [CrossRef]
20. Li, Y.; Jiang, J.-W. Modulation of Thermal Conductivity of Single-Walled Carbon Nanotubes by Fullerene Encapsulation: The Effect of Vacancy Defects. *Phys. Chem. Chem. Phys.* **2023**, *25*, 7734–7740. [CrossRef]

21. Kaur, R.; Sen, S.; Larsen, M.C.; Tavares, L.; Kjelstrup-Hansen, J.; Ishida, M.; Zieleniewska, A.; Lynch, V.M.; Bähring, S.; Guldi, D.M.; et al. Semiconducting Supramolecular Organic Frameworks Assembled from a Near-Infrared Fluorescent Macrocyclic Probe and Fullerenes. *J. Am. Chem. Soc.* **2020**, *142*, 11497–11505. [CrossRef] [PubMed]
22. Fan, J.; Chamberlain, T.W.; Wang, Y.; Yang, S.; Blake, A.J.; Schröder, M.; Khlobystov, A.N. Encapsulation of Transition Metal Atoms into Carbon Nanotubes: A Supramolecular Approach. *Chem. Commun.* **2011**, *47*, 5696–5698. [CrossRef] [PubMed]
23. Avdoshenko, S.M.; Fritz, F.; Schlesier, C.; Kostanyan, A.; Dreiser, J.; Luysberg, M.; Popov, A.A.; Meyer, C.; Westerström, R. Partial Magnetic Ordering in One-Dimensional Arrays of Endofullerene Single-Molecule Magnet Peapods. *Nanoscale* **2018**, *10*, 18153–18160. [CrossRef] [PubMed]
24. Chamberlain, T.W.; Pfeiffer, R.; Howells, J.; Peterlik, H.; Kuzmany, H.; Kräutler, B.; Ros, T.D.; Melle-Franco, M.; Zerbetto, F.; Milić, D.; et al. Engineering Molecular Chains in Carbon Nanotubes. *Nanoscale* **2012**, *4*, 7540–7548. [CrossRef] [PubMed]
25. Sato, S.; Yamasaki, T.; Isobe, H. Solid-State Structures of Peapod Bearings Composed of Finite Single-Wall Carbon Nanotube and Fullerene Molecules. *Proc. Natl. Acad. Sci. USA* **2014**, *111*, 8374–8379. [CrossRef]
26. Fergani, F.; Chadli, H.; Belhboub, A.; Hermet, P.; Rahmani, A. Theoretical Study of the Raman Spectra of C_{70} Fullerene Carbon Peapods. *J. Phys. Chem. C* **2015**, *119*, 5679–5686. [CrossRef]
27. Bandow, S.; Hiraoka, T.; Yumura, T.; Hirahara, K.; Shinohara, H.; Iijima, S. Raman Scattering Study on Fullerene Derived Intermediates Formed within Single-Wall Carbon Nanotube: From Peapod to Double-Wall Carbon Nanotube. *Chem. Phys. Lett.* **2004**, *384*, 320–325. [CrossRef]
28. Joung, S.-K.; Okazaki, T.; Kishi, N.; Okada, S.; Bandow, S.; Iijima, S. Effect of Fullerene Encapsulation on Radial Vibrational Breathing-Mode Frequencies of Single-Wall Carbon Nanotubes. *Phys. Rev. Lett.* **2009**, *103*, 027403. [CrossRef]
29. Okubo, S.; Okazaki, T.; Kishi, N.; Joung, S.-K.; Nakanishi, T.; Okada, S.; Iijima, S. Diameter-Dependent Band Gap Modification of Single-Walled Carbon Nanotubes by Encapsulated Fullerenes. *J. Phys. Chem. C* **2009**, *113*, 571–575. [CrossRef]
30. Dresselhaus, M.S.; Dresselhaus, G.; Saito, R.; Jorio, A. Raman Spectroscopy of Carbon Nanotubes. *Phys. Rep.* **2005**, *409*, 47–99. [CrossRef]
31. Chen, M.; Shen, W.; Bao, L.; Cai, W.; Xie, Y.; Akasaka, T.; Lu, X. Regioselective Thermal Reaction between Triethylamine and C_{60} Revisited: X-Ray Confirmation of the Pentane-Fused Adduct and in Situ Mechanism Study. *Eur. J. Org. Chem.* **2015**, *2015*, 5742–5746. [CrossRef]
32. Simon, F.; Kuzmany, H.; Rauf, H.; Pichler, T.; Bernardi, J.; Peterlik, H.; Korecz, L.; Fülöp, F.; Jánossy, A. Low Temperature Fullerene Encapsulation in Single Wall Carbon Nanotubes: Synthesis of N@C_{60}@SWCNT. *Chem. Phys. Lett.* **2004**, *383*, 362–367. [CrossRef]
33. Akasaka, T.; Wakahara, T.; Maeda, Y.; Kataura, H.; Maruyama, S. Processing Method of Single-Walled Carbon Nanotube. J.P. Patent No. 4792591B2, 12 October 2011.
34. Rojwal, V.; Singha, M.K.; Mondal, T.K. Amorphous Silicon and Carbon Nanotubes Layered Thin-Film Based Device for Temperature Sensing Application. *IEEE Sens. J.* **2021**, *21*, 2627–2633. [CrossRef]
35. Zeinabad, H.A.; Zarrabian, A.; Saboury, A.A.; Alizadeh, A.M.; Falahati, M. Interaction of Single and Multi Wall Carbon Nanotubes with the Biological Systems: Tau Protein and PC12 Cells as Targets. *Sci. Rep.* **2016**, *6*, 26508. [CrossRef] [PubMed]